Optimal Motion Control for Energy-aware Electric Vehicles

Tao Wang and **Christos G. Cassandras**
Division of Systems Engineering
and Center for Information and Systems Engineering
Boston University, renowang@bu.edu, cgc@bu.edu

***Abstract*— We study two problems of optimally controlling how to accelerate and decelerate a non-ideal energy-aware electric vehicle so as to (a) maximize its cruising range and (b) minimize the traveling time to a specified destination under a limited battery constraint. Modeling an electric vehicle as a dynamic system, we adopt an Electric Vehicle Power Consumption Model (EVPCM) and formulate two respective optimal motion control problems. Although the full solutions can only be obtained numerically, we propose approximate controller structures such that the original optimal control problems are transformed into nonlinear parametric optimization problems, which are much easier to solve. Numerical examples illustrate the solution structures and support their accuracy.**

I. Introduction

The emergence of plug-in hybrid electric vehicles (HEV) and fully electric vehicles (EV) is motivated by the goals of reduced oil dependency and greenhouse gas emissions. However, both HEVs and EVs heavily rely on limited battery power, thus raising such issues as vehicle cruising ranges and accessibility to charging sources.

In the HEV literature, work has been focused on designing optimal strategies for power distribution between the electric motor and the combustion engine in order to minimize fuel consumption [1], [2]. Moreover, efforts have been dedicated to establishing control-oriented models of the traction dynamics of the vehicles, which are the vital ingredients for active controllers to achieve desired accuracy and energy-efficiency. For example, a dynamic model of the powertrain of HEVs is proposed in [3]; [4] addresses the traction control of an EV; and speed and acceleration controllers are studied for an energy-aware two-wheeled EV in [5].

On the other hand, the expanding number of HEV and EV fleets brings out new research issues related to insufficient power supplied to vehicles, allocation of limited charging stations and power balance of electric grids. From the vehicle side, a circuit-based battery is commonly used to represent the electricity source when considering the supervisory control of an HEV [6]. Sundstrom et al. [7] employed this model to optimally plan the charging behaviors of EV fleets in terms of grid power balancing. In order to minimize the waiting time for EV charging, a scheduling problem in a network of EVs and charging stations was studied in [8]. From the grid side, an optimization methodology of allocating the recharging infrastructure for EVs in an urban environment was developed in [9]. More recently, a decentralized protocol for negotiating day-ahead charging schedules for EVs via pricing control was proposed in [10] to fill the overnight electricity demand valley. However, despite the variety of research on HEV/EV energy-aware systems, there is little work investigating HEV/EV motion control from a power management perspective, which is mainly because the relationship between vehicle dynamics and power consumption is complicated.

The authors' work is supported in part by NSF under Grants EFRI-0735974 and CNS-1139021, by AFOSR under grant FA9550-12-1-0113, by DOE under grant DE-FG52-06NA27490, by ONR under grant N00014-09-1-1051, and by ARO under grant W911NF-11-1-0227.

An analytical power consumption model for an EV was proposed in [11], which presents a comprehensive relationship between velocity, acceleration and power consumption rate. Motivated by this model, we formulate two optimal motion control problems, i.e., a cruising range maximization problem and a vehicular traveling time minimization. Although the intricate state dynamics of the problems require resorting to numerical solutions, they do serve to formulate approximate solution structures so as to transform the original difficult optimal control problems into simpler nonlinear parametric optimization problems. While for the first problem the solution turns out to involve practically unrealistic optimal parameter settings, for the second problem the solution does give an optimal strategy with reasonable settings. Moreover, the approximate solutions possess a much simpler structure while preserving accuracy. This approximation technique allows us to apply optimal motion planning to various interesting issues in EV-based systems, such as vehicular routing, charging station deployment and EV-to-smart-grid (V2G) charging scheduling, thus opening up a wide spectrum of research directions.

The structure of the paper is as follows. In Section II, we introduce the analytical power consumption model for EVs. In Section III, we formulate an EV cruising range maximization problem based on a power consumption model with a prescribed initial energy. The explicit numerical solution, as well as an approximate one, are presented and the accuracy of the latter is verified. Based on the approximate solution structure, the optimal control problem is reduced to a nonlinear parametric optimization problem, which is easier to solve. Section IV explores an EV traveling time minimization problem with the same procedure as Section III. Finally, conclusions and further research directions are described in Section V.

II. Electric Vehicle Power Consumption Model (EVPCM)

In [11], an analytical electric vehicle power consumption model (EVPCM) was proposed, capturing the relationship between vehicular power consumption and motion metrics (velocity, acceleration). The accuracy of this model is verified based on tests involving two real EVs. The following table is the nomenclature used for the EVPCM:

$K = \frac{K_a \phi N}{R}$	K_a : DC motor innate armature constant; ϕ : magnetic flux on the armature; R : radius of the tire $[m]$; N : gear reduction ratio
r	coil resistance [Ω]
m	vehicle mass [kg]
$a(t)$	acceleration at time t [m/s^2]
$v(t)$	vehicle velocity at time t [m/s]
k	air resistance constant [kg/m]
μ	rolling resistance constant
g	gravity acceleration constant [m/s^2]
$P(t)$	instantaneous output power of the battery at t [J]

TABLE I
NOMENCLATURE FOR THE EVPCM

This model takes into account the power consumption on vehicle traction as well as heat loss of the motor. The former part can be expressed as:

$$P_\tau(t) = v(t)F(t) = v(t)(ma(t) + kv^2(t) + mg\mu) \quad (1)$$

where $F(t)$ represents the instantaneous motor traction force, incorporating the acceleration resistance, air resistance and rolling resistance respectively (assuming the vehicle travels on flat ground so that the inclination resistance is ignored). When a vehicle motor runs at high speed, the energy loss coming from the coil heating cannot be ignored. However, this is usually not considered when modeling the vehicle's engine-generator power consumption [12]. In [11], the power loss due to the motor is modeled according to the relationship of the motor back-electromotive force $E(t)$, the motor current $I(t)$, the vehicle velocity $v(t)$ and the motor traction force $F(t)$, which are as follows:

$$\begin{cases} F(t) = \frac{K_a \phi N}{R} \cdot I(t) = KI(t) \\ E(t) = \frac{K_a \phi N}{R} \cdot v(t) = Kv(t) \end{cases}$$

resulting in $I(t) = F(t)/K$. Along with the definition of $F(t)$ in (1), the power loss due to the motor at time t becomes:

$$P_m(t) = I^2(t)r = \frac{r}{K^2}(ma(t) + kv^2(t) + mg\mu)^2$$

Therefore, the total vehicle power consumption is $P_m(t) + P_t(t)$. In other words, the instantaneous battery output power of an EV is:

$$\begin{aligned} P[a(t), v(t)] =& \frac{r}{K^2}(ma(t) + kv^2(t) + mg\mu)^2 \\ &+ v(t)(ma(t) + kv^2(t) + mg\mu) \end{aligned} \quad (2)$$

Note that it is possible to have $P[a(t), v(t)] < 0$ when $a(t) < 0$, which indicates that the EVPCM also incorporates the regenerative braking effect, i.e., the EV's battery recovering energy from braking.

III. Cruising Range Maximization Problem

A. Problem Statement

EVs usually have a smaller maximum cruising range on a single charge than cars powered by fossil fuels. Therefore, the cruising range is critical for an EV to consider before it can reach its destination or a charging station. Motivated by this issue, we seek to control the acceleration process so as to maximize the EV's cruising distance with a given initial battery power, where the EV is modeled as an EVPCM. We denote the EV's traveling distance by time t as $x(t)$ and the instantaneous battery's residual energy at time t as $e(t)$. $v(t)$ and $a(t)$ are respectively the vehicle velocity and acceleration, defined in Tab. I, and $a(t)$ is the only control variable. We let $P(t)$ be the EV's instantaneous battery output power, whose expression is given in (2). Therefore, the problem we are interested in can be formulated as a state constrained optimal control problem with an unspecified terminal time T aiming to maximize the range $x(T)$ or equivalently:

$$\min_{a(t)} \quad -x(T) \quad (3)$$

$$\dot{x}(t) = v(t) \quad (4)$$

$$\dot{v}(t) = a(t) \quad (5)$$

$$\dot{e}(t) = -P(t) \quad (6)$$

$$e(0) = E_0, \quad x(0) = 0, \quad v(0) = 0 \quad (7)$$

$$e(T) = e_{min}, \ v(T) = 0 \quad (8)$$

$$e(t) \geq 0, \quad 0 \leq v(t) \leq v_{max} \quad (9)$$

$$a_{min} \leq a(t) \leq a_{max} \quad (10)$$

where the initial conditions in (7) initialize the battery energy, traveled distance and vehicle speed. The terminal time T is determined by (8), implying that the entire process ends when the battery energy reaches a given minimum value e_{min} which, for simplicity, we take to be $e_{min} = 0$ without affecting the analysis. Finally, v_{max} bounds the top speed while a_{min} and a_{max} are, respectively, the maximum deceleration and acceleration, where $a_{min} < 0$ and $a_{max} > 0$.

B. Hamiltonian Analysis

We begin by analyzing the unconstrained case in which (9) are relaxed. In this case, the optimal state trajectory consists of an interior arc over the entire interval $[0, T]$. Let $\mathbf{x}(t) = (x(t), v(t), e(t))^T$ and $\lambda(t) = (\lambda_1(t), \lambda_2(t), \lambda_3(t))^T$ denote the state and costate vector respectively. The Hamiltonian for this problem is

$$H(\mathbf{x}, \lambda, a) = \lambda_1(t)v(t) + \lambda_2(t)a(t) - \lambda_3(t)P(a, v) \quad (11)$$

Then, the costate (Eular-Lagrange) equations $\dot{\lambda} = -\frac{\partial H}{\partial \mathbf{x}}$ give

$$\begin{cases} \dot{\lambda}_1(t) = 0 \\ \dot{\lambda}_2(t) = -\lambda_1(t) + \lambda_3(t)\frac{\partial P(a,v)}{\partial v} \\ \dot{\lambda}_3(t) = 0 \end{cases} \quad (12)$$

In view of (2), we have

$$\frac{\partial P(a,v)}{\partial v} = \frac{r}{K^2}\left(4k^2v^3(t) + 4mkv(t)a(t) + 4mg\mu kv(t)\right) + ma(t) + 3kv^2(t) + mg\mu \quad (13)$$

Moreover, due to (3) and (8), we must satisfy $\lambda(T) = \frac{\partial \Phi(\mathbf{x}(T))}{\partial \mathbf{x}}$, where $\Phi(\mathbf{x}(T)) = -x(T) + \nu_1 v(T) + \nu_2 e(T)$ and ν_1, ν_2 are unknown multipliers, so that

$$\lambda_1(T) = -1, \quad \lambda_2(T) = \nu_1, \quad \lambda_3(T) = \nu_2 \quad (14)$$

Since the terminal time is unspecified, the transversality condition $L + \frac{d\Phi}{dt}|_{t=T} = 0$ ($L = 0$ here) gives

$$-v(T) + \nu_1 a(T) - \nu_2 P[a(T), v(T)] = 0 \quad (15)$$

Note that from (14) and (12),

$$\dot{\lambda}_2(t) = 1 + \nu_2 \frac{\partial P(a,v)}{\partial v}, \quad \text{with } \lambda_2(T) = \nu_1 \quad (16)$$

where $\lambda_2(t)$ is a function of the control $a(t)$ due to (13). Therefore, in view of (11), the Hamiltonian is not a linear function of $a(t)$. As a result, we can use the optimality condition $\frac{\partial H}{\partial a} = 0$ so that

$$\lambda_2(t) - \lambda_3(t)\frac{\partial P(a,v)}{\partial a} = 0 \quad (17)$$

where

$$\frac{\partial P(a,v)}{\partial a} = \frac{rm}{K^2}\left(2ma(t) + 2kv^2(t) + 2mg\mu\right) + mv(t) \quad (18)$$

Now a two-point boundary value problem is fully specified using (12)-(18). However, owing to the complexity of $\frac{\partial P(a,v)}{\partial v}$ in (16), we are unable to analytically obtain $\lambda_2(t)$. Therefore, we have to resort to numerical methods.

C. Numerical Solution

We solve this optimal control problem by means of *GPOPS* [13], an open-source MATLAB-based optimal control solver that implements the Gauss and Radau *hp*-adaptive pseudo-spectral methods. A numerical example of the optimal solution and optimal state trajectories is shown in Fig.1. The parameter settings are listed in Tab. II and are the ones used for a 4-wheeled TOYOTA Coms [11] except that the values of E_0, a_{min} and a_{max} which we have selected.

$K_a\phi$ [V· s]	r [Ω]	R [m]	k [kg/m]	a_{min} [m/s^2]	N
1.05	0.16	0.23	1.26	-15	1
g [m/s^2]	μ	m [kg]	E_0 [J]	a_{max} [m/s^2]	
9.8	0.006	350	10^4	20	

TABLE II
PARAMETER SETTINGS FOR THE EVPCM

In Fig.1, the numerical solution displays a clear structure for the optimal acceleration: it starts with a small value (0.0588 m/s^2 in the solution), slowly decreases to 0 at some time, gradually increasing the speed up to a value (1.0338 m/s), and then remains at 0 for a while, and in the end slowly decreases to a negative value (-0.0588 m/s^2), bringing the speed down to 0. The accelerating process in the beginning and decelerating process in the end are symmetric in terms of the absolute values of acceleration and velocity. Under the control process, the energy trajectory $e(t)$ and the cruising distance $x(t)$ seem to be respectively linearly decreasing and increasing throughout $[0, T]$. In this example, $T^* = 406.7113$ s and $x^*(T) = 387.4078$ m.

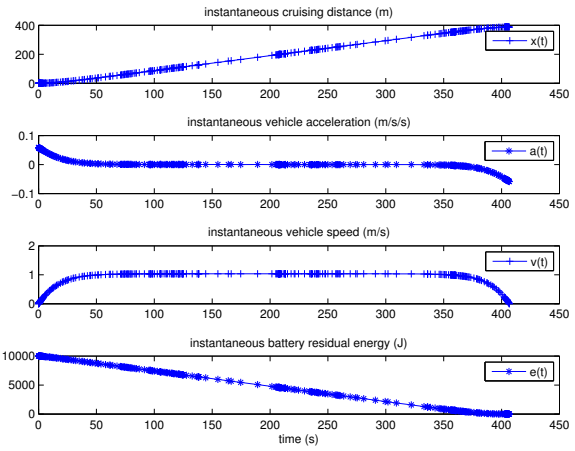

Fig. 1. Optimal solution of the Cruising Range Maximization Problem

D. Approximate Parametric Optimization Problem

Motivated by the numerical solution and its clear structure, we propose an approximate optimal control $\tilde{a}^*(t)$ as follows:

$$\tilde{a}^*(t) = \begin{cases} \frac{A}{t_1}(t_1 - t) & t \in [0, t_1] \\ 0 & t \in (t_1, t_2] \\ -\frac{A}{t_1}(t - t_2) & t \in (t_2, T] \end{cases} \quad (19)$$

where $T = t_1 + t_2$ and A, t_1 and t_2 are the unknown parameters to be determined, also satisfying $0 < A \le a_{max}$ and $0 < t_1 \le t_2$. This structure approximates the numerically obtained optimal control $a^*(t)$ by linearizing the gradually changing curves at the beginning and ending parts shown in Fig.1.

Accordingly, since the acceleration structure has been determined, the velocity structure can be obtained through (5):

$$\tilde{v}^*(t) = \begin{cases} At - \frac{A}{2t_1}t^2 & t \in [0, t_1] \\ \frac{At_1}{2} & t \in (t_1, t_2] \\ \frac{A}{t_1}(\frac{t_1^2 - t_2^2}{2} - \frac{t^2}{2} + t_2 t) & t \in (t_2, T] \end{cases} \quad (20)$$

We let $v_{cr} = \frac{At_1}{2}$, which is the critical cruising speed of the vehicle over $(t_1, t_2]$.

Moreover, in light of (4) and (7), we can write the objective function (3) as

$$\tilde{x}^*(T) = x(0) + \int_0^T \tilde{v}^*(t)dt = \frac{A}{6}(3t_1t_2 + t_1^2) \quad (21)$$

Note that since $T = t_1 + t_2$, then $\tilde{v}^*(T) = 0$ by (20), which satisfies the terminal condition (8). However, we

still have a constraint on the terminal energy value, i.e., $e(T) = 0$. Therefore, substituting $\tilde{a}^*(t)$ and $\tilde{v}^*(t)$ into (2) and integrating (6) from 0 to T, we can establish a new equality constraint $g(A, t_1, t_2) = 0$ defined by:

$$e(T) - e(0) = \int_0^T -P(t)dt \Longrightarrow$$
$$g(A,t_1,t_2) = \int_0^{t_1} \frac{r}{K^2}\Big(\frac{mA}{t_1}(t_1 - t) + k(At - \frac{A}{2t_1}t^2)^2 + mg\mu\Big)^2 + (At - \frac{A}{2t_1}t^2)\Big(\frac{mA}{t_1}(t_1 - t) + k(At - \frac{A}{2t_1}t^2)^2 + mg\mu\Big)dt + \int_{t_1}^{t_2} \frac{r}{K^2}\Big(k(\frac{At_1}{2})^2 + mg\mu\Big)^2 + \frac{At_1}{2}\Big(k(\frac{At_1}{2})^2 + mg\mu\Big)dt + \int_{t_2}^{t_1+t_2} \frac{r}{K^2}\Big(-\frac{mA}{t_1}(t - t_2) + k(\frac{A}{2t_1}(t_1^2 - t_2^2) + \frac{A}{t_1}(-\frac{t^2}{2} + t_2 t))^2 + mg\mu\Big)^2 + (\frac{A}{2t_1}(t_1^2 - t_2^2) + \frac{A}{t_1}(-\frac{t^2}{2} + t_2 t))\Big(-\frac{mA}{t_1}(t - t_2) + k(\frac{A}{2t_1}(t_1^2 - t_2^2) + \frac{A}{t_1}(-\frac{t^2}{2} + t_2 t))^2 + mg\mu\Big)dt - E_0 = 0$$

We use the software package *Mathematica* [14] to complete the integration, the result of which is presented as follows:

$$g(A,t_1,t_2) = \Big[\frac{r}{K^2}(m^2g^2\mu^2 + m^2Ag\mu + \frac{1}{3}m^2A^2)t + (\frac{mg\mu A}{3} + \frac{mA^2}{8})t^2 + \frac{r}{K^2}(\frac{1}{12}mA^3k + \frac{4}{15}mg\mu kA^2)t^3 + \frac{2}{35}kA^3t^4 + \frac{8rk^2A^4t^5}{315K^2}\Big]\Big|_0^{t_1} + \Big[\frac{r}{K^2}(\frac{k^2A^4}{16}t_1^4 + \frac{kmg\mu A^2}{2}t_1^2 + m^2g^2\mu^2) + \frac{kA^3}{8}t_1^3 + \frac{mg\mu A}{2}t_1\Big]t\Big|_{t_1}^{t_2} + \Big[\frac{r}{16K^2t_1^4}\Big(\big(A^2(t_1^2 - t_2^2)^2k + 4at_1t_2m + 4t_1^2\mu gm\big)^2 t + 4A\big(At_2(t_1^2 - t_2^2)k - t_1m\big)\big(A^2(t_1^2 - t_2^2)^2k + 4At_1t_2m + 4t_1^2\mu gm\big)t^2 - \frac{4}{3}A^2\big(A^2(t_1^2 - 7t_2^2)(t_1^2 - t_2^2)^2k^2 + 4At_1t_2(3t_1^2 - 5t_2^2)km + 4t_1^2(t_1^2\mu gk - 3t_2^2\mu gk - m)m\big)t^3 - 2A^2k\big(A^2t_2\cdot(3t_1^4 - 10t_1^2t_2^2 + 7t_2^4)k - 2At_1(t_1^2 - 5t_2^2)m + 4t_1^2t_2\mu gm\big)t^4 + \frac{2}{5}A^2k\big(A^2(3t_1^4 - 30t_1^2t_2^2 + 35t_2^4)k + 20At_1t_2m + 4t_1^2\mu gm\big)t^5 - \frac{4}{3}A^3k(-3At_1^2t_2k + 7At_2^3k + t_1m)t^6\frac{4}{7}A^4(t_1^2 - 7t_2^2)k^2t^7 - A^4t_2k^2t^8 + \frac{1}{9}A^4k^2t^9\Big) + \frac{A}{8t_1^3}\Big(-\frac{4}{3}t_1^2\mu gmt(-3t_1^2 + 3t_2^2 - 3t_2t + t^2) + At_1mt(-2t_2 + t)(-2t_1^2 + 2t_2^2 - 2t_2t + t^2) + \frac{A^2kt}{35}\big(35t_1^6 - 35t_1^4(3t_2^2 - 3t_2t + t^2) + 21t_1^2(5t_2^4 - 10t_2^3t + 10t_2^2t^2 - 5t_2t^3 + t^4) - 5(7t_2^6 - 21t_2^5t + 35t_2^4t^2 - 35t_2^3t^3 + 21t_2^2t^4 - 7t_2t^5 + t^6)\big)\Big)\Big]\Big|_{t_2}^{t_1+t_2} - E_0 = 0 \quad (22)$$

Now along with (21), we can transform the original optimal control problem into a nonlinear parametric optimization problem:

$$\min_{A,t_1,t_2} -\tilde{x}^*(T) = \frac{A}{6}(3t_1t_2 + t_1^2) \quad (23)$$
$$s.t. \quad g(A,t_1,t_2) = 0$$
$$0 < A \le a_{max}, \quad 0 < t_1 \le t_2$$

Using the same parameter settings as in Tab. II, we solve this problem using the general-purpose nonlinear optimization problem solver *KNITRO* [16]. In the numerical solution, $A^* = 0.0515$, $t_1^* = 39.2287$ and $t_2^* = 370.5033$ such that $\tilde{x}^*(T) = 387.2875$, which is a very accurate approximation of the optimal objective $x^*(T) = 387.4078$ for the optimal control problem. Fig. 2 shows the optimal solution and optimal state trajectories, closely resembling those in Fig.1.

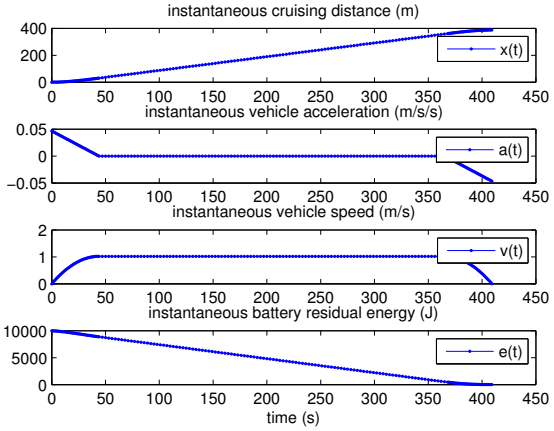

Fig. 2. Optimal solution of the parametric optimization problem

To further justify the effectiveness of our approximate solution, we compare the objective values in the solutions of the two problems based on different values of E_0 in Tab. III. The comparison shows that the solution to the parametric optimization problem is nearly equivalent to the one of the optimal control problem. In addition, the numerical solutions

	$E_0 = 10^3$	$E_0 = 5 \times 10^3$	$E_0 = 10^4$	$E_0 = 4 \times 10^4$
$x^*(T)$	34.7192	191.3058	387.4078	1.4582×10^3
$\tilde{x}^*(T)$	34.5986	191.2110	387.2875	1.4336×10^3

TABLE III
COMPARISON OF SOLUTIONS TO THE OPTIMAL CONTROL PROBLEM AND THE PARAMETRIC OPTIMIZATION PROBLEM

indicate that the maximum value of $v^*(t)$ is much lower than the value v_{max} commonly used for EVs (around 100 km/h or 28 m/s) [11]. Consequently, we can relax the state constraint $0 \le v(t) \le v_{max}$ without affecting the optimality of the solution. On the other hand, since the critical cruising speed v_{cr} is so low in the optimal solution, we also investigate the performance of the optimal solution by comparing it to other candidate solutions with different cruising speed values as shown in Fig. 3. The investigation is under the

setting $E_0 = 10^4$ (J), in which the point $(1.011, 387.3)$ is clearly the summit of the curve, also verifying that the solution at $v_{cr} = 1.011$ m/s (3.6396 km/h) achieves the maximum cruising range $x^*(T)$. Nonetheless, at least for this example, it is still the case that the optimal cruising speed is unrealistically low.

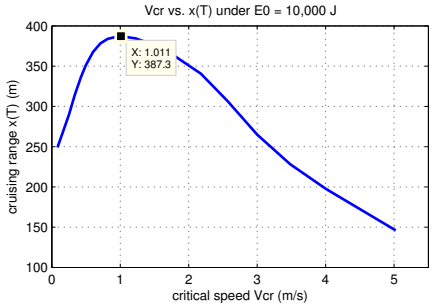

Fig. 3. Cruising range $x(T)$ vs. critical speed v_{cr} under $E_0 = 10^4$ J

To sum up, by solving the parametric problem (23) to determine the control policy (19), we obtain an approximate solution to the EV cruising range maximization problem and observe that this policy has a simple, easy to implement structure dependent only on two critical times and a fixed cruising speed maintained between these times. Admittedly, the optimal cruising speed is unreasonably low from a practical standpoint, but the approximation technique provides a means to tackle complicated optimal control problems of the same type. We will apply the same methodology to the problem of the next section, which gives more interesting results.

IV. Traveling Time Minimization Problem

A. Problem Statement

We are now interested in how fast the EV can cover a desired traveling distance with a given initial battery load. This is a traveling time minimization problem. We still adopt the EVPCM to model the EV and formulate an optimal control problem as follows:

$$\min_{a(t)} \quad \int_0^T dt \tag{24}$$

$$\dot{x}(t) = v(t) \tag{25}$$

$$\dot{v}(t) = a(t) \tag{26}$$

$$\dot{e}(t) = -P(t) \tag{27}$$

$$e(0) = E_0, \quad x(0) = 0, \quad v(0) = 0 \tag{28}$$

$$x(T) = S \tag{29}$$

$$e(t) \geq 0, \quad 0 \leq v(t) \leq v_{max} \tag{30}$$

$$a_{min} \leq a(t) \leq a_{max} \tag{31}$$

The problem formulation is almost the same as the one of the cruising range maximization problem except for the objective function (24) and the terminal condition (29), where S is the desired traveling distance, assumed to be less than the maximum achievable cruising range given the same E_0 (otherwise, there exists no feasible solution.) We also no longer require $v(T) = 0$.

B. Hamiltonian Analysis

We begin again by relaxing the state constraints (30) and analyzing the unconstrained case, where the optimal state trajectory consists of an interior arc throughout the entire process. As before, let $\mathbf{x}(t) = (x(t), v(t), e(t))^T$ and $\lambda(t) = (\lambda_1(t), \lambda_2(t), \lambda_3(t))^T$ denote the state and costate vector respectively. The Hamiltonian for this problem is

$$H(\mathbf{x}, \lambda, a) = 1 + \lambda_1(t)v(t) + \lambda_2(t)a(t) - \lambda_3(t)P(a, v) \tag{32}$$

and the costate equations $\dot{\lambda} = -\frac{\partial H}{\partial \mathbf{x}}$ are the same as (12):

$$\begin{cases} \dot{\lambda}_1(t) = 0 \\ \dot{\lambda}_2(t) = -\lambda_1(t) + \lambda_3(t)\frac{\partial P(a,v)}{\partial v} \\ \dot{\lambda}_3(t) = 0 \end{cases} \tag{33}$$

where $\frac{\partial P(a,v)}{\partial v}$ is the same as (13). Moreover, due to (3) and (8), we must satisfy $\lambda(T) = \frac{\partial \Phi(\mathbf{x}(T))}{\partial \mathbf{x}}$, where $\Phi(\mathbf{x}(T)) = \nu(x(T) - S)$ and ν are an unknown multiplier, so that

$$\lambda_1(T) = \nu, \quad \lambda_2(T) = 0, \quad \lambda_3(T) = 0 \tag{34}$$

Solving (33) with the boundary conditions (34), we get

$$\begin{cases} \lambda_1(t) = \nu \\ \lambda_2(t) = -\nu(t - T) \\ \lambda_3(t) = 0 \end{cases} \tag{35}$$

Still owing to the unspecified terminal time, the transversality condition $L + \frac{d\Phi}{dt}|_{t=T} = 0$ ($L = 1$ here) requires that

$$1 + \nu v(T) = 0 \tag{36}$$

Thus, with the terminal costate condition (34), we have

$$\nu = -\frac{1}{v(T)}$$

It follows that $\nu < 0$ with $v(T) \geq 0$, which makes $\lambda_2(t) < 0$ over $[0, T)$. We can now apply the Pontryagin minimum principle using (32):

$$H(\mathbf{x}^*, \lambda^*, a^*) = \min_{a(t)} H(\mathbf{x}, \lambda, a) \tag{37}$$

where $a^*(t)$, $t \in [0, T)$, denotes the optimal control. We can then see that since $\lambda_2(t) < 0$ and $\lambda_3(t) = 0$ over $[0, T)$,

$$a^*(t) = a_{max}, \quad t \in [0, T] \tag{38}$$

which is the optimal control policy for the unconstrained case. Accordingly, the optimal velocity trajectory is achieved by (26):

$$v^*(t) = a_{max}t, \quad t \in [0, T] \tag{39}$$

and the optimal objective value is attained by $\int_0^{T^*} v^*(t)dt = S$ in (29), which gives

$$T^* = \sqrt{\frac{2S}{a_{max}}} \tag{40}$$

When it comes to the constrained case with only $0 \leq v(t) \leq v_{max}$ incorporated, we can directly check whether

the constraint is active or not by comparing $a_{max}T^*$ with v_{max}: if $a_{max}T^* \leq v_{max}$, then the constraint is not active, therefore (38) is still the optimal control policy; otherwise, the constraint $v(t) \leq v_{max}$ is active at $t = \frac{v_{max}}{a_{max}}$ and the optimal control (38) cannot apply anymore. In this case, we can still carry out the Hamiltonian analysis. We can immediately exclude $v(T) < v_{max}$ since, if this holds, then no change would occur from (32) to (36), hence the optimal control would still be (38). Now with $v(T) = v_{max}$, we have a different $\Phi(\mathbf{x}(T)) = \nu_1(x(T) - S) + \nu_2(v(T) - v_{max})$ (ν_i are the unknown multipliers), which implies that

$$\lambda_1(T) = \nu_1, \quad \lambda_2(T) = \nu_2, \quad \lambda_3(T) = 0 \tag{41}$$

In view of (33), as long as $\lambda_3(t) = 0$, $\frac{\partial P(t)}{\partial v}$ will not be involved in $\dot{\lambda}_2(t)$, which will make $\lambda_2(t)$ independent of the control $a(t)$. Therefore, we can proceed with a similar derivation to (35)-(38) and determine the optimal control as:

$$a^*(t) = \begin{cases} a_{max}, & t \in [0, \frac{v_{max}}{a_{max}}] \\ 0, & t \in (\frac{v_{max}}{a_{max}}, T^*] \end{cases} \tag{42}$$

where T^* can be determined by (25)-(26) as:

$$T^* = \frac{S}{v_{max}} + \frac{v_{max}}{2a_{max}} \tag{43}$$

Lastly, let us consider the constrained case with both $0 \leq v(t) \leq v_{max}$ and $e(t) \geq 0$ incorporated. Regarding the optimal controls (38) and (42), $a^*(t) \geq 0$ throughout $[0, T^*]$. Then, according to (27) and (2), $P^*(t) > 0$ over $[0, T^*]$ and $e^*(t)$ is monotonically decreasing. Thus, we only need to check the value of $e^*(T)$ for the two possible optimal controls (38) and (42). If $e^*(T) \geq 0$ under the optimal control, then the constraint $e(t) \geq 0$ is not involved during $t \in [0, T)$. Otherwise, we have to revise the Hamiltonian analysis letting $\Phi(\mathbf{x}(T)) = \nu_1(x(T) - S) + \nu_2(v(T) - v_{max}) + \nu_3 e(T)$ (ν_i are the unknown multipliers), which will make $\lambda_3(T) = \nu_3$. As a result, from (33) $\lambda_2(t)$ becomes a function of $a(t)$. Similar to the analysis of the cruising range maximization problem, this analysis cannot generally yield an explicit analytical solution for the optimal control problem, so that we once again proceed with numerical solutions.

C. Numerical Solution

Since we are to address the case where the optimal controls (38) and (42) cannot apply, we assume $e(T) = 0$. At first, we relax the state constraint $v(t) \leq v_{max}$. As in Section III, by using *GPOPS* we can obtain a numerical solution to this optimal control problem. A numerical example of the optimal solution and optimal state trajectories is shown in Fig. 4. The parameter settings are the same as in Tab. II except that the required traveling distance S is set as 2000 m and the value of E_0 is 10^8, which is designed to achieve a higher top speed so as to incorporate state constraint $v(t) \leq v_{max}$ in what follows. Also, we still employ the commonly used v_{max} value, which is 28 m/s (100.8 km/h).

From Fig. 4, it is clear that in the numerical solution, the whole acceleration process consists of five parts: (1) fully accelerating at a_{max} (20 m/s^2); (2) gradually descending

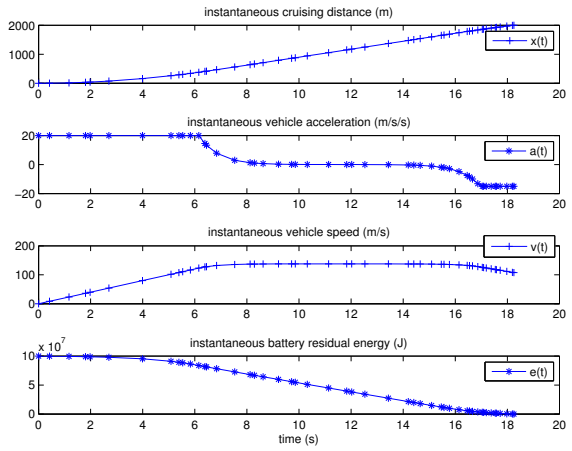

Fig. 4. Optimal solution to the Traveling Time Minimization Problem

to 0; (3) maintaining $a(T) = 0$; (4) gradually descending to the maximum decelerating value a_{min} (-15 m/s^2) and (5) fully decelerating at a_{min} to the end. Accordingly, along with the acceleration process the speed increases until it reaches part (3), and then remains at a fixed value until some time after which the vehicle is required to fully decelerate for the remaining traveling time. Under this optimal control, we obtain $T^* = 18.2523$s.

Moreover, in this numerical example, we notice that the maximum velocity value is 137.5064 m/s (about 495 km/h), which is unrealistically high in practice. However, note that this result is only for the relaxed problem without incorporating v_{max}, and usually $v_{max} < 137.5064$ m/s. By numerically perturbing the value of v_{max} we find that there exist two additional types of solutions. The first one can be expressed as

$$a_1^*(t) = \begin{cases} a_{max}, & t \in [0, \frac{v_{max}}{a_{max}}] \\ 0, & t \in (\frac{v_{max}}{a_{max}}, t_s] \\ a_{min} & t \in (t_s, T] \end{cases} \tag{44}$$

in which case $e(T) = 0$ and the value of t_s depends on v_{max} and E_0. The second one arises when v_{max} and E_0 are such that $t_s = T$ in (44) but $e(T) > 0$, in which case the solution is the same as (42). This case corresponds to a scenario where the vehicle has so much initial energy that it can complete the entire process as fast as possible with a positive residual energy.

D. Approximate Parametric Optimization Problem

Motivated by the results obtained in the last section, we can again propose an approximate optimal control $\tilde{a}^*(t)$ as follows:

$$\tilde{a}^*(t) = \begin{cases} a_{max} & t \in [0, t_1] \\ 0 & t \in (t_1, t_2] \\ a_{min} & t \in (t_2, T] \end{cases} \tag{45}$$

where t_1, t_2 and T are unknown parameters to be determined, also satisfying $0 < t_1 \leq t_2 \leq T$ and $t_1 \leq \frac{v_{max}}{a_{max}}$. This

control structure contains all three types of optimal controls obtained through numerical solutions.

Accordingly, the velocity structure can be expressed using (5):

$$\tilde{v}^*(t) = \begin{cases} a_{max}t & t \in [0, t_1] \\ a_{max}t_1 & t \in (t_1, t_2] \\ a_{max}t_1 + a_{min}(t - t_2) & t \in (t_2, T] \end{cases} \tag{46}$$

Therefore, in light of (25) and (28), we can represent the terminal condition (29) by a new equality constraint:

$$g_1(t_1, t_2, T) = a_{max}t_1(T - \frac{t_1}{2}) + \frac{a_{min}(T - t_2)^2}{2} - S = 0 \tag{47}$$

Moreover, as pointed out earlier, the condition $e^*(T) > 0$ could only occur in the optimal solution (42). Thus, we can simply check the feasibility of the solution (42): if, under (42), $e(T) > 0$, then the optimal solution is (42); otherwise, we can add the additional terminal condition $e(T) = 0$ without affecting the solution.

Thus, let us assume $e(T) = 0$ in what follows. Substituting $\tilde{a}^*(t)$ and $\tilde{v}^*(t)$ into (2) and integrating (6) from 0 to T, we can replace the condition $e(T) = 0$ with an equality constraint $g_2(t_1, t_2, T) = 0$, where $g(t_1, t_2, T)$ is:

$$\begin{aligned} &e(T) - e(0) = \int_0^T -P(t)dt \Longrightarrow \\ &g_2(t_1, t_2, T) = \int_0^{t_1} \frac{r}{K^2}(ma_{max} + ka_{max}^2t^2 + mg\mu)^2 + \\ &a_{max}t(ma_{max} + ka_{max}^2t^2 + mg\mu)dt + \int_{t_1}^{t_2} \frac{r}{K^2}(ka_{max}^2t_1^2 \\ &+ mg\mu)^2 + a_{max}t_1(ka_{max}^2t_1^2 + mg\mu)dt + \\ &\int_{t_2}^{T} \frac{r}{K^2}\Big(ma_{min} + k\big(a_{max}t_1 + a_{min}(t - t_2)\big)^2 + mg\mu\Big)^2 \\ &(a_{max}t_1 + a_{min}(t - t_2))\Big(ma_{min} + \\ &k\big(a_{max}t_1 + a_{min}(t - t_2)\big)^2 + mg\mu\Big)dt \end{aligned}$$

As in the previous section, we use *Mathematica* to do the integration, the result of which is as follows:

$$\begin{aligned} &g_2(t_1, t_2, T) = \Bigg[\frac{r}{K^2}\Big((ma_{max} + mg\mu)^2t + \frac{2}{3}(ma_{max} + \\ &mg\mu)ka_{max}^2t^3 + frack^2a_{max}^4 5t^5\Big) + \frac{1}{2}(ma_{max}^2 + \\ &mg\mu a_{max})t^2 + \frac{ka_{max}^3}{4}t^4\Bigg]\Bigg|_0^{t_1} + \Big[\frac{r}{K^2}(ka_{max}^2t_1^2 + mg\mu)^2 + \\ &a_{max}t_1(ka_{max}^2t_1^2 + mg\mu)\Big]t\Big|_{t_1}^{t_2} + \Bigg[\frac{r}{K^2}\Big(\big(mg\mu + a_{max}^2t_1^2k - \\ &2a_{min}a_{max}t_2k + a_{min}(a_{min}t_2^2k + m)\big)^2t - 2a_{min}\cdot \\ &(-a_{max}t_1 + a_{min}t_2)k\big(mg\mu + a_{max}^2t_1^2k - 2a_{min}a_{max}t_1t_2k \\ &+ a_{min}(a_{min}t_2^2k + m)\big)t^2 + \frac{2}{3}a_{min}^2k\big(mg\mu + 3a_{max}^2t_1^2k - \\ &6a_{min}a_{max}t_1t_2k + a_{min}(3a_{min}t_2^2k + m)\big)t^3 - \\ &a_{min}^2(-a_{max}t_1 + a_{min}t_2)k^2t^4 + \frac{1}{5}a_{min}^4k^2t^5\Big) + \\ &\frac{1}{4}t\big(2a_{max}t_1 + a_{min}(-2t_2 + t)\big)\Big(2mg\mu + 2a_{max}^2t_1^2k + \\ &2a_{min}a_{max}t_1k(-2t_2 + t) + \\ &a_{min}\big(2m + a_{min}k(2t_2^2 - 2t_2t + t^2)\big)\Big)\Bigg]\Bigg|_{t_2}^{T} - E_0 = 0 \end{aligned} \tag{48}$$

Now, along with (47), we can transform the original optimal control problem into a nonlinear parametric optimization problem as follows:

$$\begin{aligned} \min_{t_1, t_2, T} \quad & T \\ s.t. \quad & g_1(t_1, t_2, T) = 0 \\ & g_2(t_1, t_2, T) = 0 \\ 0 < t_1 \le t_2 \le T, \quad & t_1 \le \frac{v_{max}}{a_{max}} \end{aligned} \tag{49}$$

Note that the constraint $t_1 \le \frac{v_{max}}{a_{max}}$ is equivalent to $v \le v_{max}$. Using the same parameter settings as in the optimal control problem, we use *KNITRO* to solve this problem. In order to verify the accuracy of our approximate solution, we first relax the constraint $t_1 \le \frac{v_{max}}{a_{max}}$ and compare the result with the numerical solution in Fig. 4. In the solution to the parametric problem (49), $t_1^* = 6.6369$ s and $T^* = t_2^* = 18.3858$ s, which can be seen to be very close to the numerical optimal objective $T^* = 18.2523$ s for the optimal control problem. Fig. 5 shows the solution and corresponding state trajectories.

If we incorporate the constraint $t_1 \le \frac{v_{max}}{a_{max}}$ with $v_{max} = 28$ m/s (about 100 km/h, the usual v_{max} values for EVs mentioned earlier), then we apply the control policy (42) and test the corresponding $e(T)$, which turns out to be 9.6706×10^7 J, much greater than 0. Consequently, (42) is the optimal control in this case, under which $T^* = 72.1000$ s. The solution, including the control and state trajectories, is shown in Fig. 6. If we reduce the initial energy E_0, then the optimal top speed will correspondingly decrease. Thus, when E_0 is small enough, the optimal top speed does not exceed the speed limit v_{max}. In this scenario, the optimal controller behaves as (45) and the solution is shown in Fig.

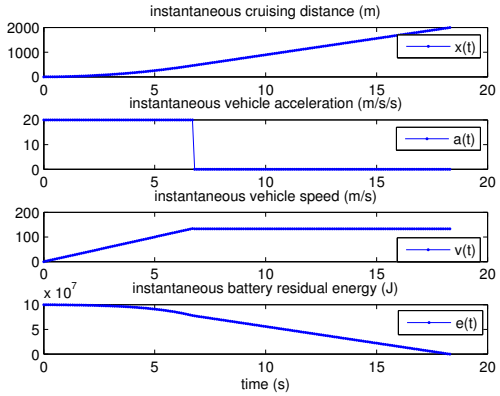

Fig. 5. Optimal solution to the parametric optimization problem without the constraint $t_1 \leq \frac{v_{max}}{a_{max}}$

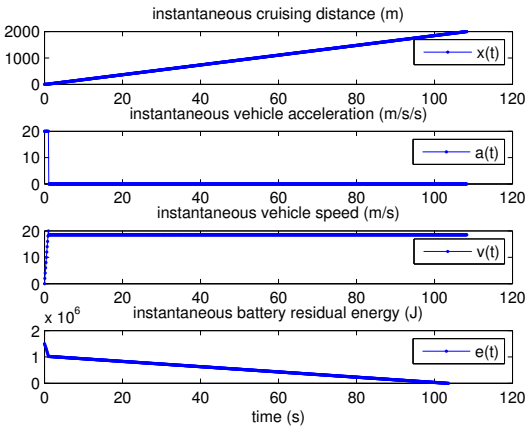

Fig. 7. Optimal solution to the parametric optimization problem without violating $t_1 \leq \frac{v_{max}}{a_{max}}$

7, where the optimal cruising speed is 18.5342 m/s (about 67 km/h). Unlike the range maximization problem, this optimal speed is reasonable for EVs.

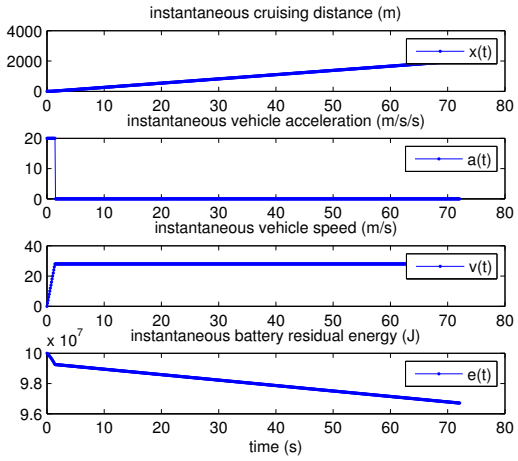

Fig. 6. Optimal solution to the parametric optimization problem with $t_1 \leq \frac{v_{max}}{a_{max}}$

V. Conclusions and Future Work

We have used an Electric Vehicle Power Consumption Model (EVPCM) to study two problems of optimally controlling the acceleration (and deceleration) of a non-ideal energy-aware electric vehicle so as to (a) maximize the cruising range and (b) minimize the traveling time to a prescribed destination with limited battery power. In the cruising range maximization problem, due to the complicated relationship between power consumption and vehicle dynamics, the solution can only be attained numerically. However, based on the numerical solution, an approximate solution structure is proposed such that the original optimal control problem can be transformed into a nonlinear parametric optimization problem, which is easier to solve. The accuracy of the approximate solution is also verified. Even though the speed values involved in the optimal solution for this problem are practically unrealistic, the approach provides a methodology to solve complicated optimal control problems of this type, where the vehicle state dynamics are too complex for exact analytical solutions to be derived. Subsequently using this methodology to the traveling time minimization problem yields interesting and practically realizable results. For both problems, we have obtained simple near-optimal solution structures despite the complexity of an elaborate vehicle energy consumption model.

This line of research opens up a wide spectrum of extensions. With the approximate simple solution structure for both problems, we can integrate the EVPCM into a number of problems including vehicular routing, charging station deployment and EV to smart grid (V2G) charging scheduling, where either EV traveling time or distance are metrics to optimize over.

References

[1] A. Sciarretta, M. Back, and L. Guzzella, "Optimal control of parallel hybrid electric vehicles," *IEEE Transactions on Control Systems Technology*, vol. 12, no. 3, pp. 352–363, 2004.

[2] F. Salmasi, "Control strategies for hybrid electric vehicles: Evolution, classification, comparison, and future trends," *IEEE Transactions on Vehicular Technology*, vol. 56, no. 5, pp. 2393–2404, 2007.

[3] B. Powell, K. Bailey, and S. Cikanek, "Dynamic modeling and control of hybrid electric vehicle powertrain systems," *IEEE Control Systems Magazine*, vol. 18, no. 5, pp. 17–33, 2002.

[4] Y. Hori, Y. Toyoda, and Y. Tsuruoka, "Traction control of electric vehicle: Basic experimental results using the test ev uot electric march," *IEEE Transactions on Industry Applications*, vol. 34, no. 5, p. 1131C1138, 2002.

[5] A. Dardanelli, M. Tanelli, B. Picasso, S. M. Savaresi, O. di Tanna, and M. Santucci, "Optimal decentralized protocols for electric vehicle charging," in *50th IEEE Conf. on Decision and Control*, Orlando, FL, Dec. 2011.

[6] L. Guzzella and A. Sciarretta, *Vehicle Propulsion Systems: Introduction to Modeling and Optimization*. 2nd Ed. Berlin: Springer, 2007.

[7] O. Sundstrom and C. Binding, "Opimization methods to plan the charging of electric vehicle fleets," in *50th IEEE Conf. on Decision and Control*, Orlando, FL, Dec. 2011.

[8] H. Qin and W. Zhang, "Charging scheduling with minimal waiting in a network of electric vehicles and charging stations," in *VANET '11 Proceedings of the Eighth ACM international workshop on Vehicular inter-networking*, New York, NY, 2011.

[9] J. Gallego and E. Larrodeg, "Efficient allocation of recharging stations for electric vehicles in urban environments," in *Advanced Microsystems for Automotive Applications, VDI-Buch 2011*, 2011, pp. 49–58.

[10] L. Gan, U. Topcu, and S. Low, "Optimal decentralized protocols for electric vehicle charging," in *50th IEEE Conf. on Decision and Control*, Orlando, FL, Dec. 2011.

[11] D. Tanaka, T. Ashida, and S. Minami, "An analytical method of ev velocity profile determination from the power consumption of electric vehicles," in *IEEE Vehicle Power and Propulsion Conference (VPPC)*, Harbin, China, Sept. 2008.

[12] Z. Taha, R. Passarella, N. A. Rahim, and J. M. Sah, "Driving force characteristic and power consumption of 4.75 kw permanent magnet motor for a solar vehicle," *ARPN Journal of Engineering and Applied Sciences*, vol. 5, no. 1, p. 26C31, 2010.

[13] A. V. Rao, C. L. Darby, D. Garg, G. T. Huntington, D. A. Benson, M. Patterson, B. Mahon, and C. Francolin, "http://www.gpops.org."

[14] Wolfram Research Inc., "http://www.wolfram.com/mathematica."

[15] Ziena Optimization Inc. and Tomlab Optimization, "TOMLAB/KNITRO v5.1," 2007.